

~~CONFIDENTIAL~~

~~CLASSIFICATION CANCELLED~~
DATE: OCT 22 1954
BY: [illegible]

NACA RM SE54J06



RESEARCH MEMORANDUM

for the

Bureau of Aeronautics, Department of the Navy

PRELIMINARY ALTITUDE PERFORMANCE DATA OF J71-A2

TURBOJET ENGINE AFTERBURNER

By James W. Useller and William E. Mallett

Lewis Flight Propulsion Laboratory
Cleveland, Ohio

Restriction/Classification

Cancelled

This material contains information of the espionage laws, Title 18, U.S.C., in such a manner to unauthorized person

the United States within the meaning of the espionage laws, Title 18, U.S.C., in such a manner to unauthorized person

NATIONAL ADVISORY COMMITTEE FOR AERONAUTICS

WASHINGTON

FILE COPY

To be returned to the Office of the Director

In Aeronautics
Washington, D.C.

~~CONFIDENTIAL~~
DATE: OCT 22 1954
BY: [illegible]

18

CLASSIFICATION CANCELLED
CONFIDENTIAL
AUTHORITY: NASA PUBLICATIONS
ANNOUNCEMENTS NO.
Date _____ By _____

NATIONAL ADVISORY COMMITTEE FOR AERONAUTICS

RESEARCH MEMORANDUM

for the

Bureau of Aeronautics, Department of the Navy
PRELIMINARY ALTITUDE PERFORMANCE DATA OF J71-A2
TURBOJET ENGINE AFTERBURNER

By James W. Useller and William E. Mallett

SUMMARY

The performance and operational characteristics of the J71-A2 turbojet-engine afterburner were investigated for a range of altitudes from 23,000 to 60,000 feet at a flight Mach number of 0.9 and at flight Mach numbers of 0.6, 0.9, and 1.0 at an altitude of 45,000 feet. The combustion performance and altitude operational limits, as well as the altitude starting characteristics have been determined.

INTRODUCTION

At the request of the Bureau of Aeronautics, Department of the Navy, an investigation of the performance and operational characteristics of the J71-A2 turbojet engine afterburner was undertaken in an NACA Lewis laboratory altitude test chamber. A prior investigation of the unaugmented performance of the J71-A2 engine is reported in reference 1.

The afterburner performance was investigated for a range of altitudes from 23,000 to 60,000 feet at a flight Mach number of 0.9 and for flight Mach numbers of 0.6, 0.9, and 1.0 at an altitude of 45,000 feet and is presented herein. The combustion temperature and efficiency of the afterburner have been determined for a range of altitudes at a flight Mach number of 0.9. The operational limits of maximum altitude, lean blow-out, and maximum equivalence ratio have been determined, as well as the altitude starting characteristics of the afterburner.

APPARATUS AND PROCEDURE

Afterburner configuration. - The J71-A2 afterburner has a nominal length of 11 feet and diameter of 40 inches. A schematic diagram of

CLASSIFICATION CANCELLED
CONFIDENTIAL
AUTHORITY: NASA PUBLICATIONS

REF 1

T-20

the afterburner showing the location of the various components is presented in figure 1. A photograph of the afterburner and engine installed in the altitude test chamber is shown in figure 2. A sketch of the afterburner showing the ignitors, flame holder, and fuel spray system is shown in figure 3(a).

Two afterburner ignitors were located 180° apart immediately downstream of the turbine outlet. The ignitor was a tube with seven orifices equally spaced radially. A photograph of one of the ignitors is shown in figure 3(b). Ignition was accomplished by providing a momentary supply of fuel through the orifices. For comparative purposes, an NACA "hot-streak" ignitor was also used during this investigation. The NACA ignitor consisted of a single atomizing nozzle which supplied a momentary burst of fuel into a localized region of the combustor immediately upstream of the turbine.

The afterburner fuel system consisted of 22 dual spray bars (shown in fig. 3(c)) equally spaced circumferentially at a station 8.5 inches upstream of the flame holder. Each portion of the dual spray bar was separately manifolded and provided with a flow divider that controlled the fuel distribution according to the pressure necessary for good atomization. During this investigation the fuel-flow rates and supply pressures were such that only the primary segment of each spray bar was used.

The flame holder was of the 2-ring, staggered V-gutter type, and blocked 30 percent of the annular area. A sketch of the flame holder is shown in figure 3(a). The average gas velocity at the afterburner inlet was 370 feet per second.

The afterburner cooling liner was corrugated to increase its strength and was perforated from the flame holder to a distance 32 inches downstream of the flame holder. Cooling air ducted from the turbine discharge flowed through the perforated section of the afterburner wall into the combustion chamber. The afterburner exhaust nozzle had a continuously variable area that ranged from approximately 2.5 to 4.5 square feet. An afterburner control system consisting of an amplifier and a servo-valve actuator continually adjusted the exhaust-nozzle area to maintain a maximum turbine discharge gas temperature of 1670° R as indicated by the manufacturer's thermocouples.

Engine and installation. - The afterburner investigated is an integral part of the J71-A2 turbojet engine. The investigation was conducted in an NACA altitude test chamber in which pressures and temperatures simulating altitude flight conditions were supplied to the engine inlet. Altitude pressures were simulated at the engine exhaust.

The engine has a bifurcated inlet, a 16-stage, axial-flow compressor, a canular-type combustor, and a 3-stage turbine. The engine has a

nominal unaugmented thrust rating of 10,200 pounds while operating at a rotor speed of 6100 rpm and a turbine discharge gas temperature of 1670° R as indicated by the manufacturer's thermocouples.

Fuel conforming to MIL-F-5624a (grade JP-4) specification was used in both the engine and the afterburner. The lower heating value of the fuel was 18,700 Btu per pound and the hydrogen-carbon ratio was 0.169.

Instrumentation. - The afterburner inlet conditions were surveyed by 25 total-pressure and 25 total-temperature probes in addition to 12 manufacturer's thermocouples. When an average gas temperature of 1670° R was indicated by the manufacturer's thermocouples, the more complete survey with the 25 NACA thermocouples averaged only 1620° R. The cooling air-flow rate was measured in the afterburner cooling shroud by four total-pressure probes and a single stream static-pressure probe. A water-cooled rake at the exhaust-nozzle inlet containing 14 total-pressure probes placed on centers of equal area provided a survey of the afterburner exhaust conditions. The ejector passage was instrumented with nine total-pressure, three static-pressure, and three thermocouple probes.

Standard engine instrumentation was provided to measure the air flow, engine fuel flow, and thrust. A detailed description of the engine instrumentation is contained in reference 1.

Procedure. - The afterburner performance was investigated at the following simulated flight conditions with the engine operating at rated rotor speed and turbine discharge gas temperature.

<u>Altitude, ft</u>	<u>Flight Mach number</u>
23,000	0.9
35,000	0.9
45,000	0.6, 0.9, 1.0
55,000	0.9
60,000	0.9

Data were obtained at each flight condition for a range of equivalence ratios (percent of stoichiometric fuel-air ratio) from approximately 0.2 to 1.0. The range of afterburner fuel-air operation as limited by the control system was determined. Also, the maximum and minimum range of operation of the afterburner with the control system removed was investigated.

The lean limit was established by cessation of the combustion, while the rich limit was imposed by the maximum area of the exhaust nozzle. Data were obtained at these flight conditions both with and without the exhaust-nozzle ejector in position. Afterburner ignition was attempted at each flight condition with the manufacturer's ignitor and the NACA "hot-streak" ignitor.

A list of the symbols used in this report is contained in appendix A and an explanation of the method of calculations is presented in appendix B.

DATA PRESENTATION

The experimental data are grouped according to the index presented in table I. The over-all engine-afterburner performance in terms of augmented net thrust ratio and specific fuel consumption is presented in figure 4. The afterburner performance is presented in figures 5 and 6. To obtain sufficient data to compute the combustion temperature and efficiency of figure 6, it was necessary to remove the ejector configuration. It was therefore possible to evaluate the jet thrust loss imposed by installation of the ejector; this ejector-induced thrust loss is shown in figure 7.

Afterburner operational characteristics are shown in figures 8 to 10. The maximum operable altitude and range of operable equivalence ratio are shown in figure 8. The limits of operation imposed by the afterburner control system have been included on the figure to permit comparison with the region of operation possible with manual throttle control.

The afterburner altitude starting limits using the manufacturer's ignitor and the NACA "hot-streak" ignitor are compared in figure 9. The afterburner operational limits have been superimposed on this figure.

Representative longitudinal temperature distributions along the afterburner shell are shown in figure 10. The decrease in wall temperature approximately 90 inches downstream of the burner inlet is due to the cooling provided by the exhaust-nozzle ejector. The ejector cooling flow was approximately 1.5 percent of engine flow, and the afterburner internal shell cooling flow rate was between 3 and 6 percent of the engine air flow.

A tabulation of the performance data obtained in this investigation is presented in table II.

Lewis Flight Propulsion Laboratory
National Advisory Committee for Aeronautics
Cleveland, Ohio, October 7, 1954

APPENDIX A

SYMBOLS

The following symbols are used in this report:

C_j	nozzle flow coefficient
F_e	unaugmented engine net thrust, lb
F_j	augmented jet thrust, lb
F_n	augmented net thrust, lb
f/a	fuel-air ratio
g	acceleration due to gravity, 32.17 ft/sec ²
M	Mach number
P	total pressure, lb/sq ft abs
p	static pressure, lb/sq ft abs
R	gas constant, $\frac{1546 \text{ ft-lb}}{(\text{molecular wt})(\text{lb})(^\circ\text{R})}$
sfc	specific fuel consumption, lb/hr/lb
T	total temperature, $^\circ\text{R}$
V	velocity, ft/sec
W_a	air flow, lb/sec
W_f	fuel flow, lb/hr
W_g	weight flow, lb/sec
γ	ratio of specific heats
η	efficiency
ϕ	equivalence ratio

Subscripts:

ab afterburner
e engine
0 free stream
2 compressor inlet
3 compressor outlet
5 turbine outlet
9 exhaust-nozzle inlet

2557

APPENDIX B

CALCULATIONS

Equivalence ratio. - The afterburner equivalence ratio is defined as the percent of stoichiometric fuel-air ratio in the afterburner where the afterburner fuel-air ratio is defined as follows:

$$\left(\frac{f}{a}\right)_{ab} = \frac{\frac{W_{f,e} + W_{f,ab}}{W_{a,5}} - \left(\eta_e \frac{W_{f,e}}{W_{a,5}}\right)}{1 - \left[\frac{\eta_e \left(\frac{W_{f,e}}{W_{a,5}}\right)}{0.0674}\right]} \quad (1)$$

The equivalence ratio is then

$$\phi = \frac{(f/a)_{ab}}{0.0674} \quad (2)$$

where 0.0674 is the stoichiometric fuel-air ratio for the fuel used.

Augmented thrust ratio. - The augmented thrust ratio is based on the normal thrust of the standard engine configuration, afterburner not operating, as calculated at the same turbine-outlet conditions as the augmented thrust and introducing the 5.5-percent loss in total pressure caused by the drag in the afterburner. For the case of augmented net thrust the function is as follows:

$$F_n/F_e = \frac{\text{Net thrust with afterburning}}{\text{Normal net thrust}} \quad (3)$$

Over-all specific fuel consumption. - The over-all specific fuel consumption is based on the augmented net thrust and the sum of the engine and afterburner fuels.

Combustion efficiency. - The combustion efficiency of the afterburner was determined as a ratio of the actual to ideal temperature rise across the afterburner. The actual combustion temperature T_g was calculated

from the gas flow, the measured thrust, and a pressure survey at station 9, using the jet thrust equation as follows:

$$T_9 = \left(\frac{F_j}{W_{g,9}} \right)^2 \left(\frac{g}{C_j \sqrt{gR}} \right)^2 \left(\frac{V}{\sqrt{gRT}} \right)^{\frac{1}{2}} \quad (4)$$

Values of the effective velocity parameter $\left(\frac{V}{\sqrt{gRT}} \right)$ were obtained from reference 2 using the appropriate values for γ_9 . The combustion efficiency defining equation is as follows:

$$\eta_{ab} = \frac{\Delta T_{5-9}(\text{actual})}{\Delta T_{5-9}(\text{ideal})} \quad (5)$$

where the ideal temperature rise was determined by the method of reference 3.

REFERENCES

1. Useller, James W., and Mallett, William E.: Preliminary Altitude Performance Data for the J71-A2 (X-26) Turbojet Engine. NACA RM SE54H06, 1954.
2. Turner, L. Richard, Addie, Albert N., and Zimmerman, Richard H.: Charts for the Analysis of One-Dimensional Steady Compressible Flow. NACA TN 1419, 1948.
3. Mulready, Richard C.: The Ideal Temperature Rise Due to the Constant Pressure Combustion of Hydrocarbon Fuels. M.I.T. Meteor Rep. UAC-9, Res. Dept., United Aircraft Corp., July 1947. (BuOrd Contract NORD 9845.)

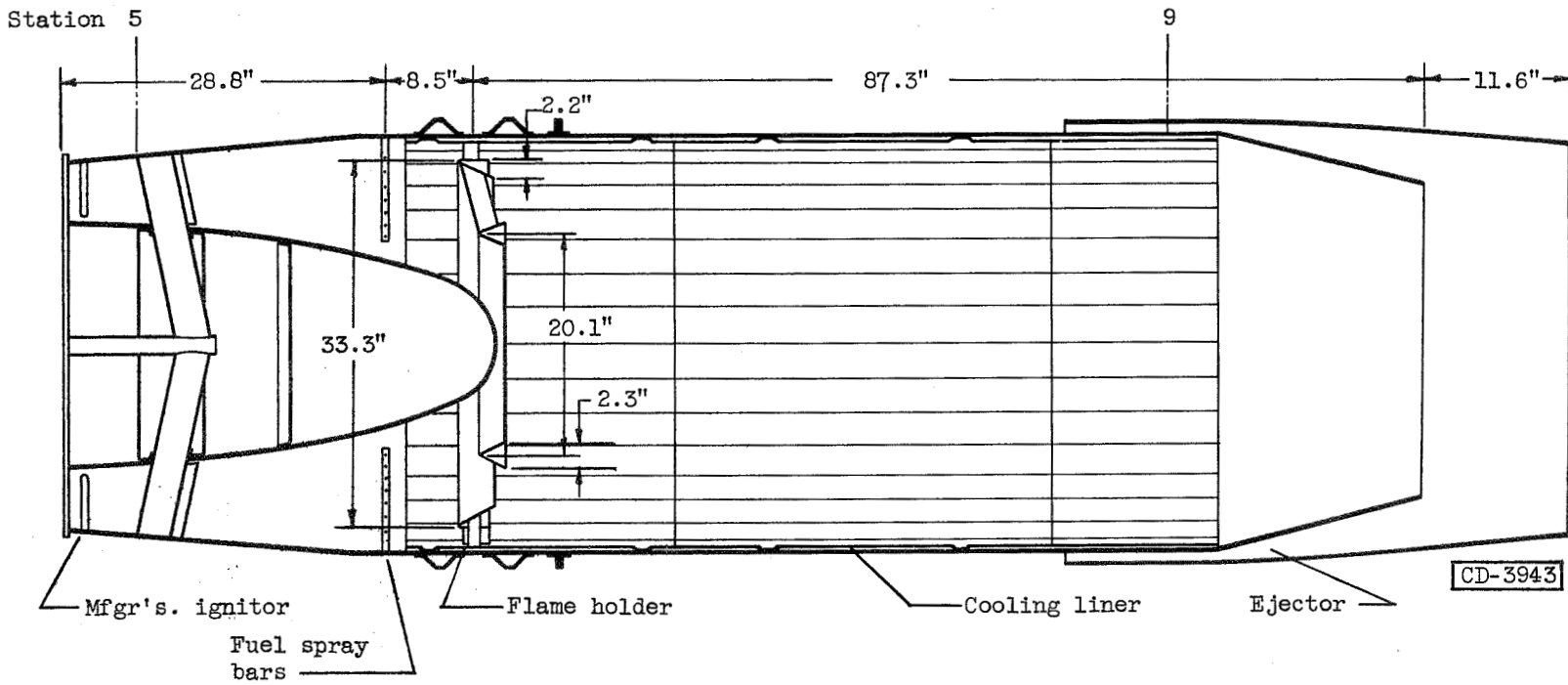
TABLE I. - FIGURE INDEX

Figure	Dependent variable	Independent variable
1	Schematic diagram of afterburner	
2	Photograph of afterburner installation	
3(a)	Afterburner component parts; flame holder and spray bars in position	
3(b)	Manufacturer's afterburner ignitor	
3(c)	Afterburner fuel spray bar	
Over-all Engine Performance		
4(a)	Augmented net thrust ratio variation with altitude	Afterburner equivalence ratio
4(b)	Over-all net thrust specific fuel consumption variation with altitude	Afterburner equivalence ratio
4(c)	Augmented net thrust ratio variation with flight Mach number	Afterburner equivalence ratio
4(d)	Over-all net thrust specific fuel consumption variation with flight Mach number	Afterburner equivalence ratio
Afterburner Performance		
5	Afterburner total pressure loss	Afterburner equivalence ratio
6(a)	Combustion temperature	Afterburner equivalence ratio
6(b)	Combustion efficiency	Afterburner equivalence ratio
Effect of Ejector on Performance		
7	Ejector jet thrust loss	Afterburner equivalence ratio
Operational Characteristics		
8	Afterburner operational limits	Afterburner equivalence ratio
9	Afterburner ignition limits	Afterburner equivalence ratio
10	Local afterburner shell temperature	Distance downstream from turbine outlet

53-4

TABLE II. - ALTITUDE PERFORMANCE DATA OF J71-A2 TURBOJET ENGINE-AFTERBURNER.

Run	Sea level altitude, ft	Nominal Mach number, M ₀	Altitude pressure, P ₀ , lb/sq ft abs	Engine inlet total pressure, P ₂ , lb/sq ft abs	Engine inlet total temperature, T ₂ , °R	Compressor total pressure, P ₃ , lb/sq ft abs	Compressor total temperature, T ₃ , °R	Turbine inlet total pressure, P ₅ , lb/sq ft abs	Turbine outlet total temperature, T ₅ , °R	Nozzle inlet total pressure, P ₉ , lb/sq ft abs	Cooling air flow, W _a , lb/sec	Engine air flow, W _e , lb/hr	Engine fuel flow, W _f , lb/hr	Afterburner fuel flow, W _{ab} , lb/hr	Augmented jet thrust, F _j , lb	Augmented net thrust, F _n , lb
With ejector configuration																
1	23,000	0.9	891	1495	541	11,360	1033	3218	1633	2984	798	108.12	5780	6,715	9,865	6669
2			889	1500	539	11,309	1028	3211	1627	2970	719	108.74	5760	7,145	10,089	6855
3			892	1502	541	11,362	1033	3203	1632	2944	754	109.33	5820	8,820	10,549	7335
4			889	1501	539	11,310	1029	3187	1628	2907	805	108.98	5710	12,050	11,198	7855
5			890	1496	541	11,359	1033	3205	1631	2918	756	108.09	5800	13,450	11,453	8249
6			894	1494	540	11,346	1030	3200	1630	2892	757	108.10	5760	15,815	11,740	8554
7			895	1503	541	11,378	1033	3235	1646	2966	809	108.19	5840	17,990	12,067	8867
8	35,000	0.9	503	824	456	7,283	939	2157	1565	2032	781	69.46	3885	3,000	5,996	4134
9			509	826	459	7,223	947	2069	1637	1935	802	69.39	3930	3,615	6,209	4363
10			508	825	460	7,229	948	2052	1645	1905	835	69.36	3910	4,830	6,731	4676
11			509	824	461	7,228	947	2056	1637	1867	873	69.22	3910	5,990	7,015	5173
12			503	---	---	---	948	2071	1641	1909	915	---	3930	6,090	---	---
13			507	825	460	7,218	947	2064	1639	1900	810	69.42	3955	7,275	7,274	5418
14			507	837	464	7,241	952	2067	1641	1888	856	69.62	3930	8,445	7,714	5714
15			507	826	459	7,261	947	2063	1638	1887	857	69.36	3955	8,460	7,516	5664
16			---	829	456	7,255	944	---	1630	---	869	70.13	3930	9,730	---	---
17			505	834	466	7,186	954	2052	1638	1866	929	68.33	3955	9,750	7,561	5724
18	45,000	0.6	305	385	422	3,572	910	1004	1646	924	919	33.75	2034	1,950	2,954	2336
19			305	386	425	3,565	910	1002	1650	915	1018	33.64	2034	2,940	3,254	2640
20			305	384	425	3,541	913	999	1646	910	1017	33.50	2034	3,420	3,306	2696
21			308	386	423	3,568	913	1008	1647	915	1035	33.70	2034	4,005	3,415	2808
22			308	385	422	3,570	911	1003	1645	910	1013	33.63	2045	4,510	3,479	2969
23			304	386	422	3,569	910	1004	1646	911	991	33.83	2040	5,100	3,585	2994
24			304	385	431	3,510	918	995	1644	897	1035	33.33	2003	5,750	3,537	2919
25	45,000	0.9	315	518	462	4,456	946	1282	1649	1193	866	42.84	2415	2,095	3,802	2640
26			310	471	461	4,471	947	1250	1650	1157	923	42.11	2460	2,115	3,779	2645
27			312	512	458	4,453	938	1311	1651	1199	887	42.26	2472	3,540	4,231	3098
28			311	517	461	4,467	947	1270	1651	1172	940	42.83	2466	3,790	4,586	3208
29			312	513	463	4,406	948	1272	1643	1161	917	42.17	2460	4,635	4,450	3313
30			312	517	460	4,444	947	1265	1650	1163	908	42.82	2460	4,830	4,578	3407
31			312	512	463	4,449	949	1263	1646	1147	909	42.31	2443	5,040	4,511	3477
32			317	516	458	4,490	943	1270	1651	1162	935	42.82	2469	5,900	4,595	3547
33			315	510	465	4,410	953	1253	1648	1133	903	41.75	2415	6,820	4,818	3502
34			317	517	466	4,478	945	1261	1648	1153	802	43.16	2495	7,110	4,820	3661
35	45,000	1.0	305	573	473	4,866	958	1365	1631	1259	904	46.42	2670	3,085	4,603	3193
36			305	575	475	4,860	960	1354	1634	1246	899	46.57	2642	4,130	4,945	3526
37			305	573	473	4,838	958	1366	1634	1246	1030	46.28	2659	5,045	5,078	3672
38	50,000	0.9	244	399	463	3,450	953	979	1650	901	892	32.50	1924	1,190	2,665	1796
39			250	397	455	3,529	948	1046	1646	911	886	33.08	1945	1,735	2,915	2059
40			243	399	463	3,469	952	982	1651	891	979	32.70	1924	2,800	3,223	2343
41			250	397	463	3,464	955	961	1647	877	980	32.74	1918	3,295	3,273	2420
42			245	399	463	3,440	955	976	1646	875	955	32.65	1929	3,705	3,394	2525
43			251	399	464	3,467	955	976	1650	892	1016	32.76	1918	4,200	3,404	2551
44			253	399	464	3,481	955	978	1647	875	943	32.67	1924	5,040	3,484	2638
45			254	399	462	3,479	955	977	1650	874	852	32.75	1935	5,910	3,502	2659
46	55,000	0.9	174 ^a	317	449	2,805	988	781	1658	723	932	26.61	1580	1,295	2,329	1609
47			186 ^a	316	465	2,726	967	753	1655	682	936	26.01	1540	1,830	2,424	1720
48			189 ^a	316	453	2,776	953	764	1650	696	967	26.44	1565	2,460	2,666	1854
49			186 ^a	316	460	2,733	968	759	1648	690	934	26.14	1535	2,549	2,549	1841
50			215 ^a	316	454	2,754	952	767	1646	698	939	26.36	1565	2,170	2,530	1814
51			199 ^a	315	458	2,745	961	753	1653	685	987	25.95	1545	2,835	2,662	1963
52			229 ^a	317	461	2,745	960	761	1651	679	985	25.91	1545	2,940	2,653	1963
53			198 ^a	316	452	2,808	962	775	1653	693	963	26.60	1580	3,415	2,984	2166
54			206 ^a	316	453	2,799	956	768	1653	692	915	26.38	1575	3,950	2,892	2182
55	60,000	0.9	162 ^a	246	461	2,181	966	586	1646	541	948	20.30	1220	1,240	1,802	1862
56			163 ^a	247	461	2,164	966	580	1646	527	915	15.75	1225	1,560	1,875	1918
57			203 ^a	254	462	2,180	968	584	1651	532	969	20.94	1246	1,650	1,956	1979
58			165 ^a	246	463	2,129	969	566	1646	511	962	20.16	1194	1,835	1,936	1997
59			158 ^a	247	468	2,146	974	585	1648	511	961	20.01	1190	2,020	1,991	1458
60			205 ^a	248	461	2,046	968	582	1649	514	989	20.41	1221	2,310	2,068	1514
61			173 ^a	248	467	2,166	974	570	1648	513	994	20.08	1204	2,325	2,027	1490
62			173 ^a	247	462	2,162	969	582	1649	523	982	20.19	1225	2,625	2,133	1593
Without ejector configuration																
63	23,000	0.9	895	1520	549	11,130	1036	3159	1638	2906	---	105.78	5670	8,150	10,285	7050
64			895	1519	552	11,078	1040	3161	1639	2886	---	105.97	5640	10,080	10,715	7518
65			895	1526	555	11,051	1044	3117	1637	2831	---	105.78	5575	12,140	11,086	7882
66			899	1522	556	11,093	1048	3119	1639	2821	---	105.58	5620	14,185	11,326	8140
67			899	1522	554	11,081	1043	3128	1643	2817	---	105.34	5620	16,500	11,547	8571
68	35,000	0.9	497	834	459	7,297	941	2112	1649	1948	---	69.35	4015	5,260	7,114	5219
69			490	832	460	7,304	942	2103	1644	1925	---	69.26	3995	7,280	7,619	5700
70			494	839	461	7,329	943	2110	1647	1919	---	69.65	4015	9,220	8,014	6084
71			494	834	462	7,274	943	2099	1639	1900	---	69.28	3995	11,170	8,159	6244



CD-3943

Figure 1. - Schematic diagram of J71-A2 turbojet engine afterburner showing location of various components.

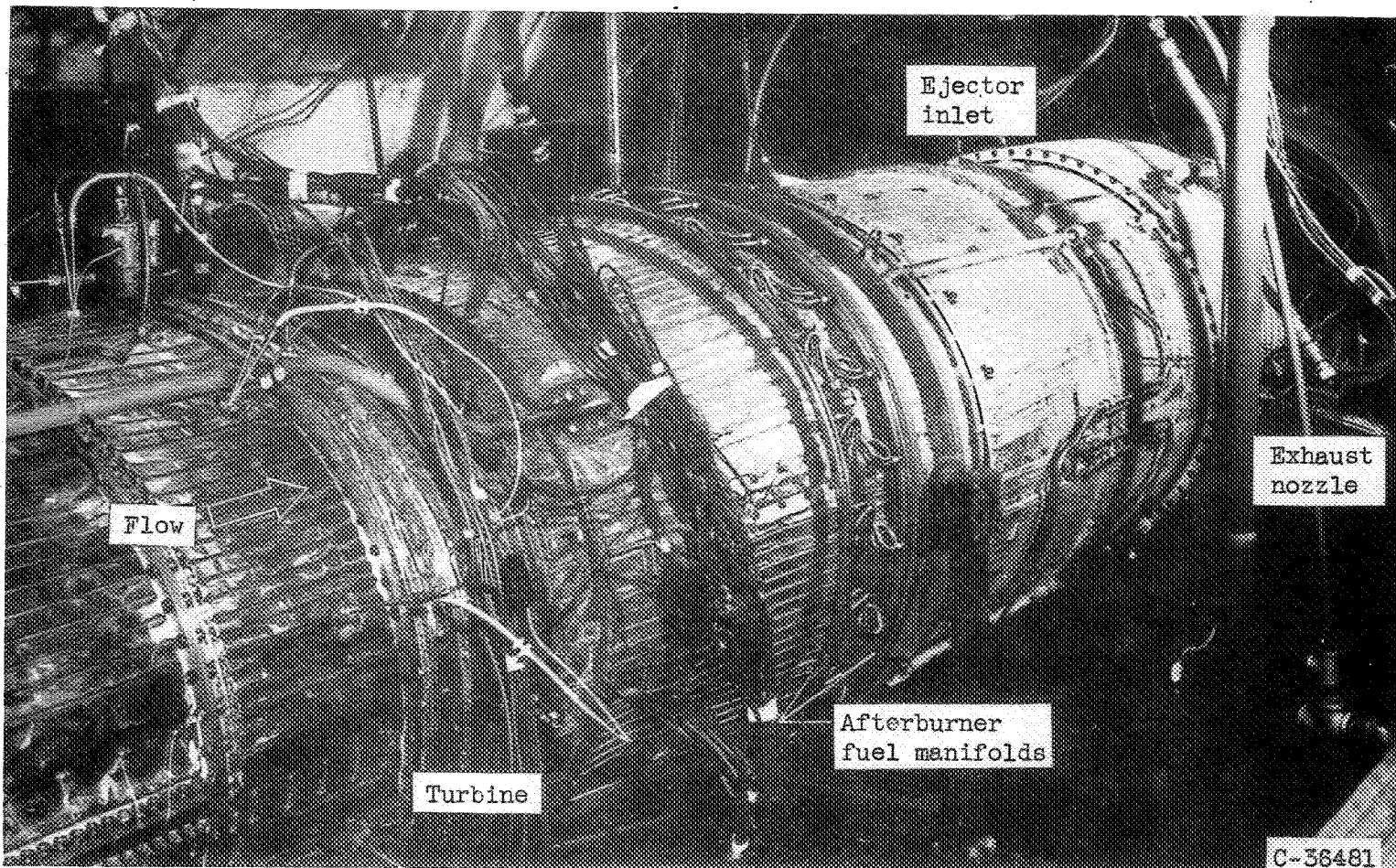
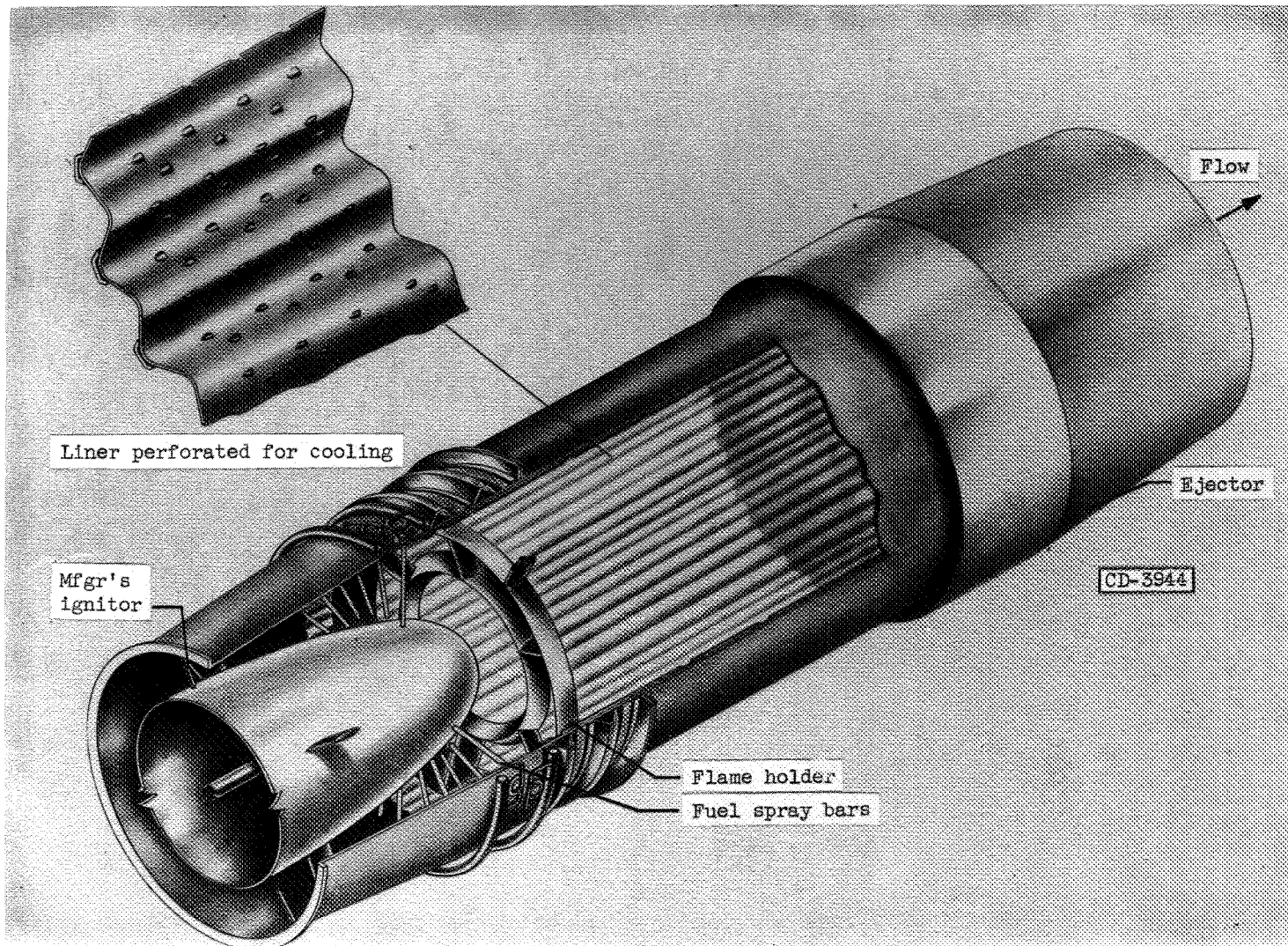
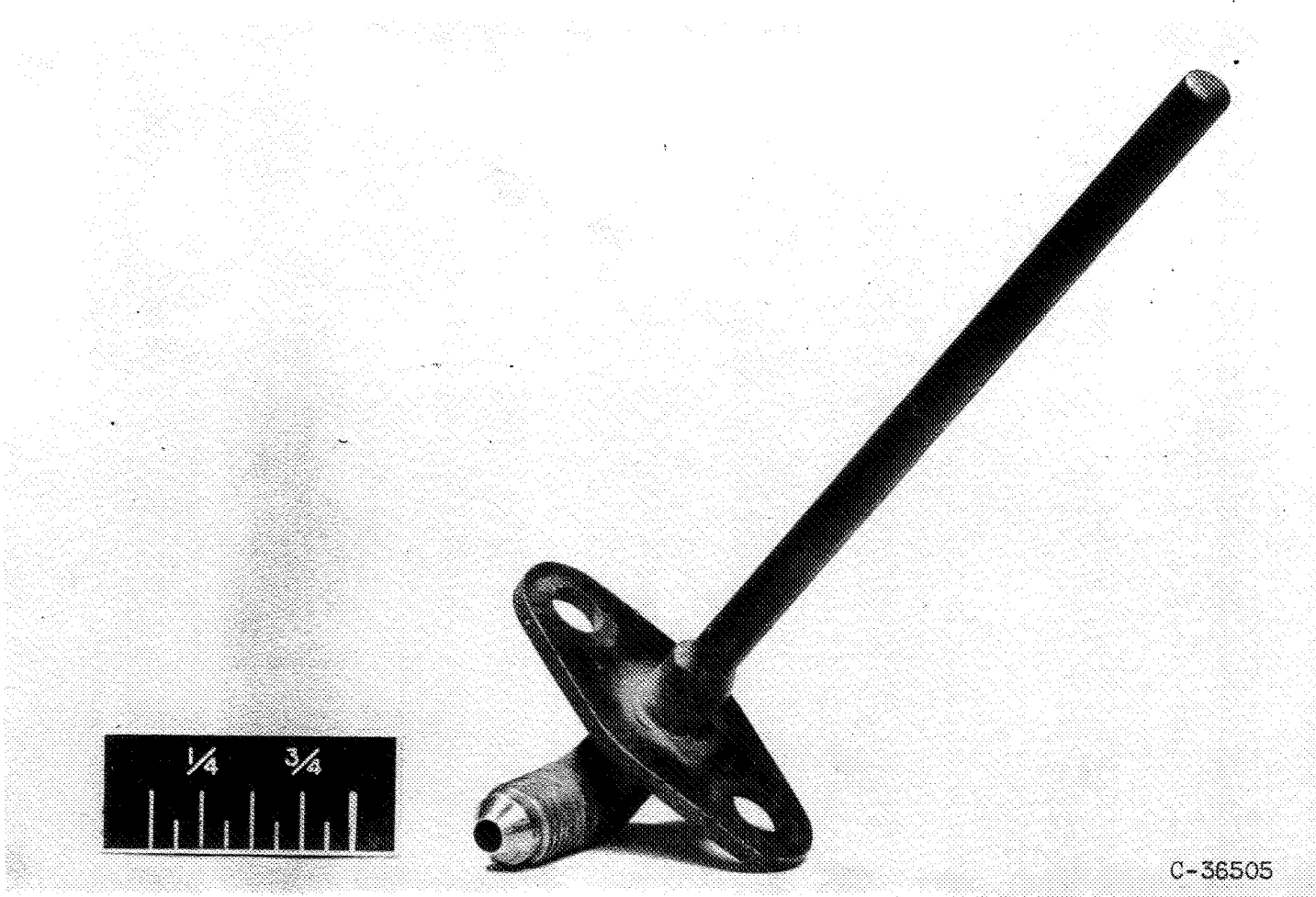


Figure 2. - J71-A2 turbojet engine afterburner installed in altitude test chamber.



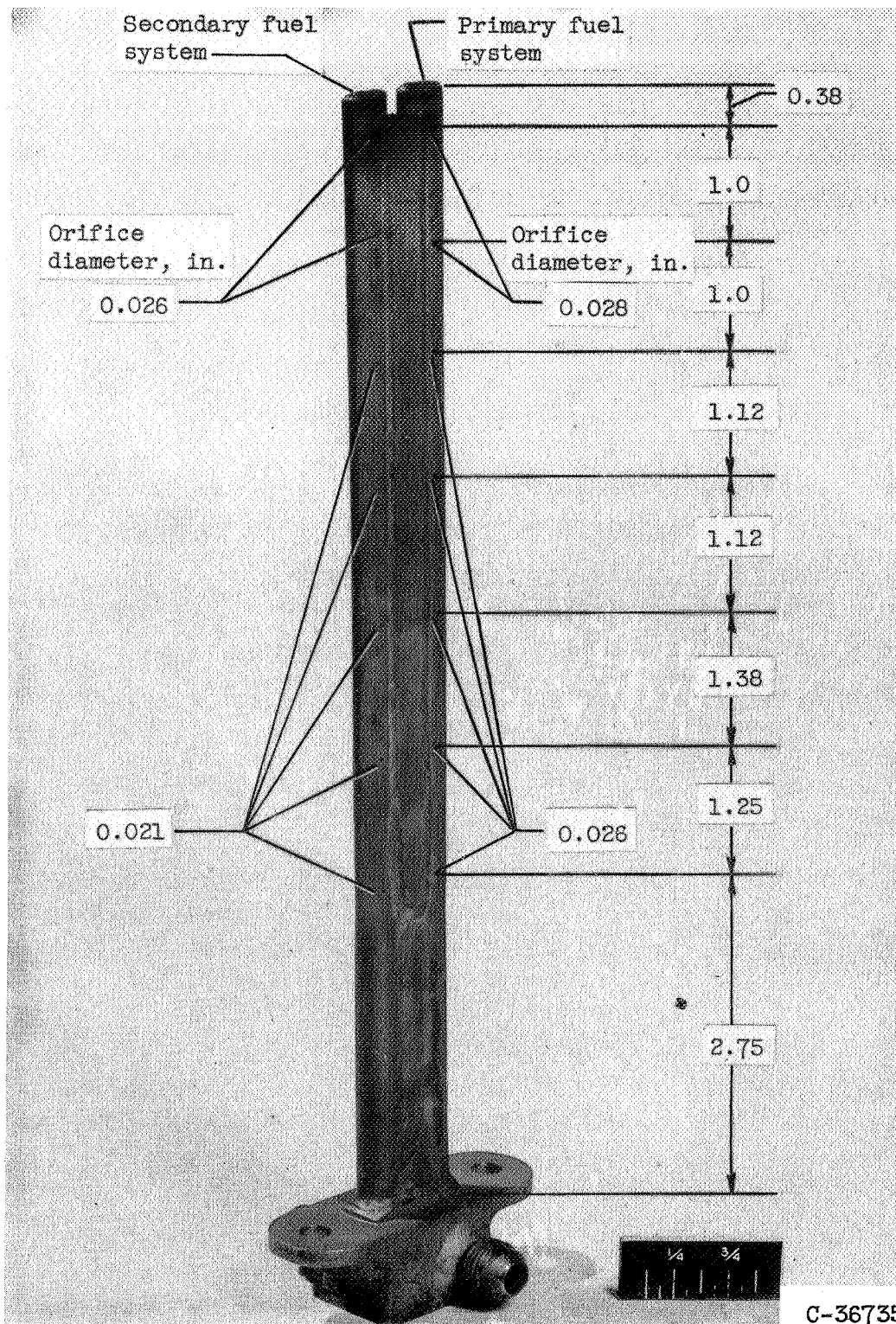
(a) Sketch showing afterburner flame holder and spray bars in position.

Figure 3. - J71-A2 turbojet engine afterburner component parts.



(b) Manufacturer's afterburner ignitor.

Figure 3. - Continued. J71-A2 turbojet engine afterburner component parts.



(c) Afterburner fuel spray bar.

Figure 3. - Concluded. J71-A2 turbojet engine afterburner component parts.

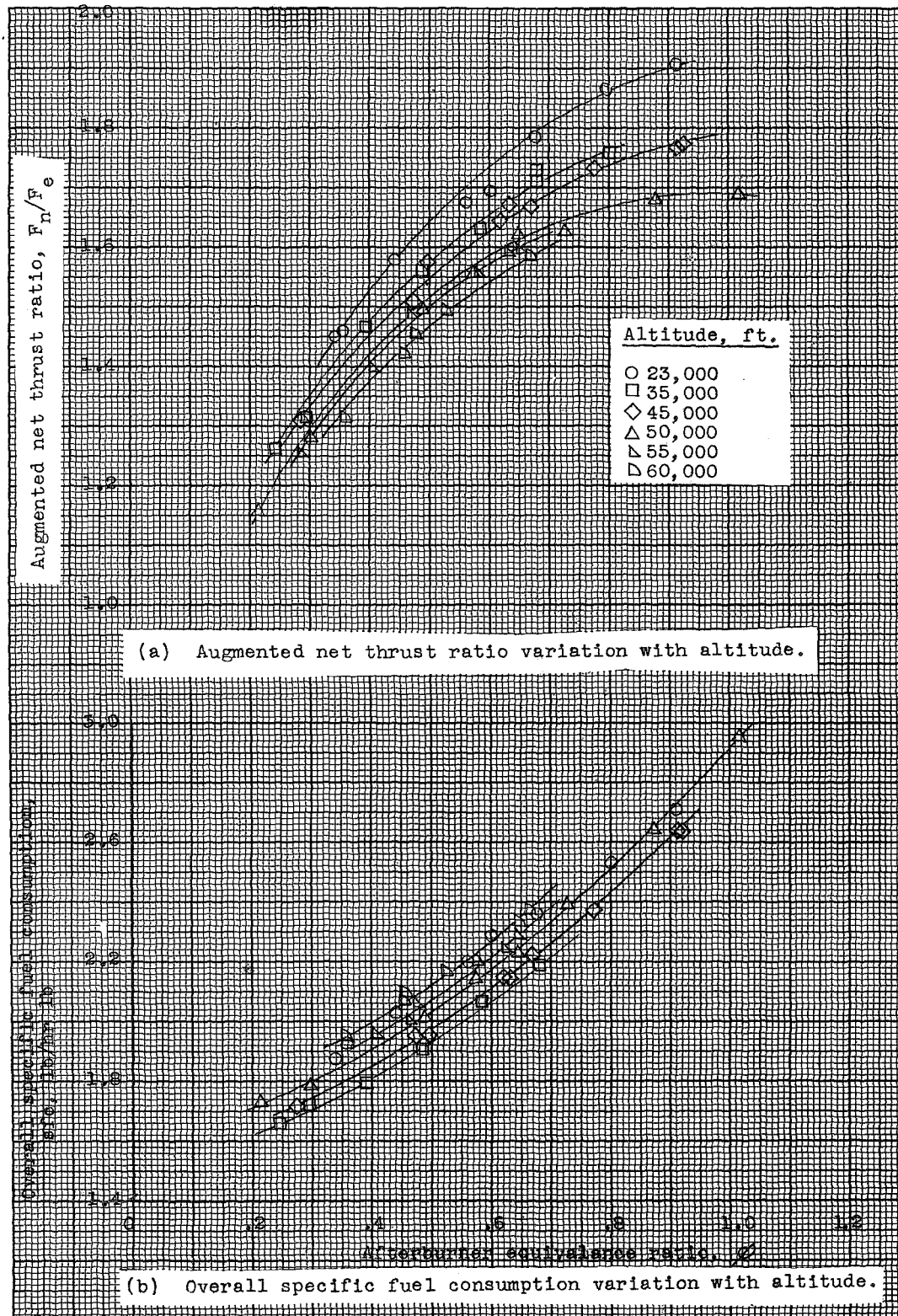
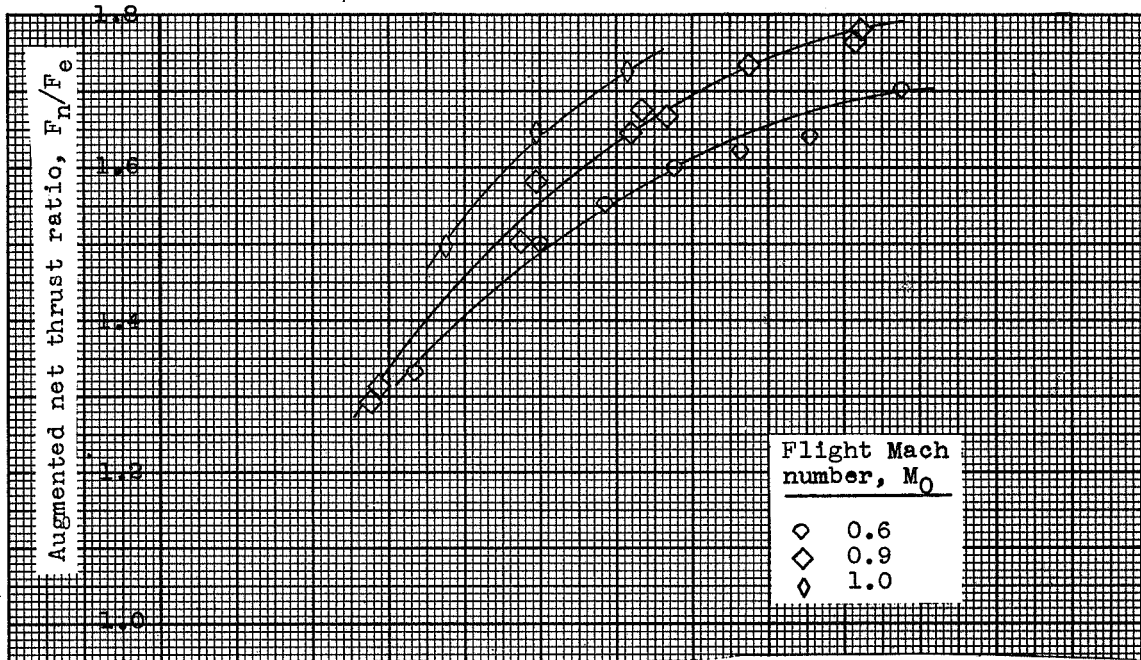
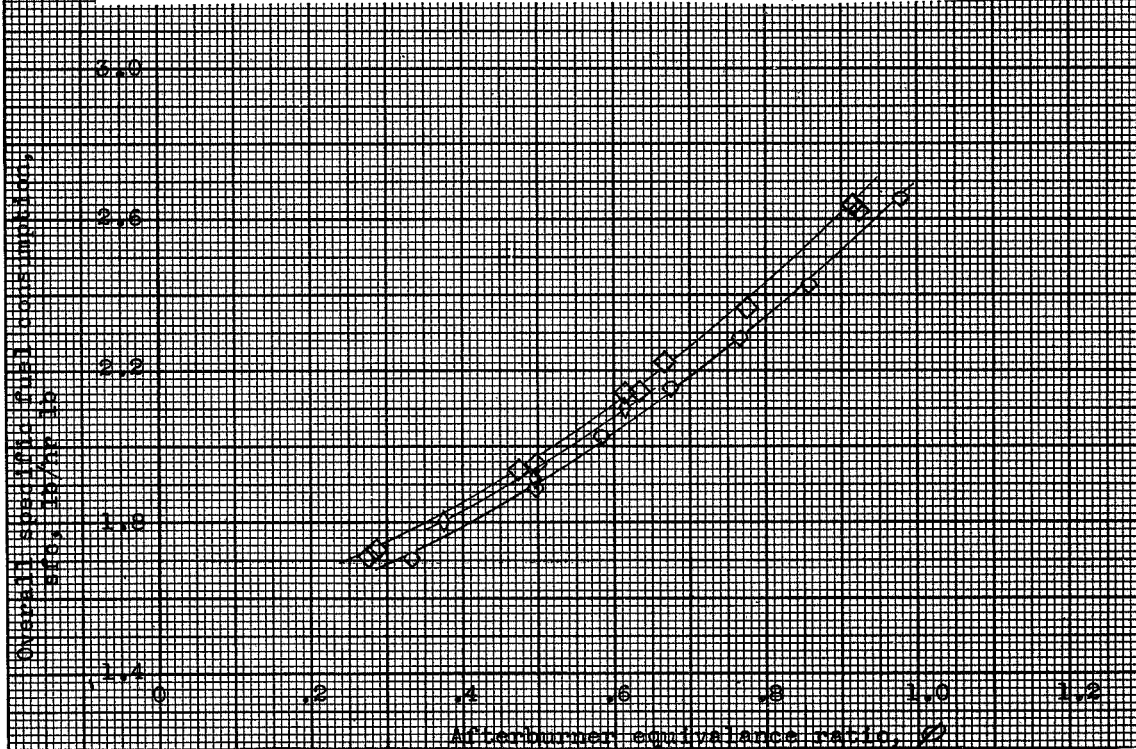


Figure 4. J71-A2 turbojet engine afterburner performance variation with altitude and flight Mach number.



(c) Augmented net thrust ratio variation with flight Mach number.



(d) Overall specific fuel consumption variation with flight Mach number.

Figure 4. J71-A2 turbojet engine afterburner performance variation with altitude and flight Mach number.

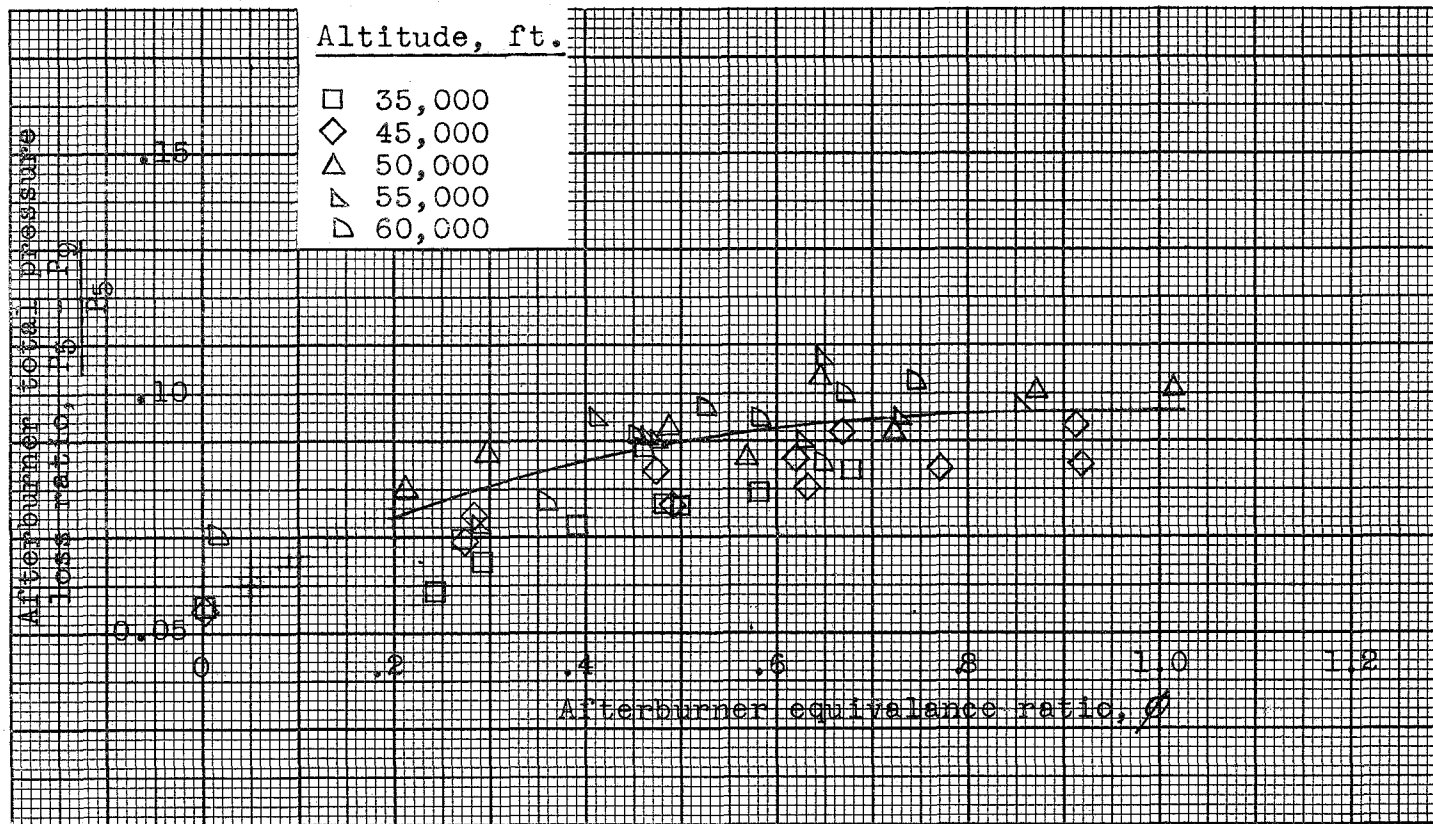


Figure 5. J71-A2 turbojet engine afterburner total pressure loss variation with afterburner equivalence ratio.

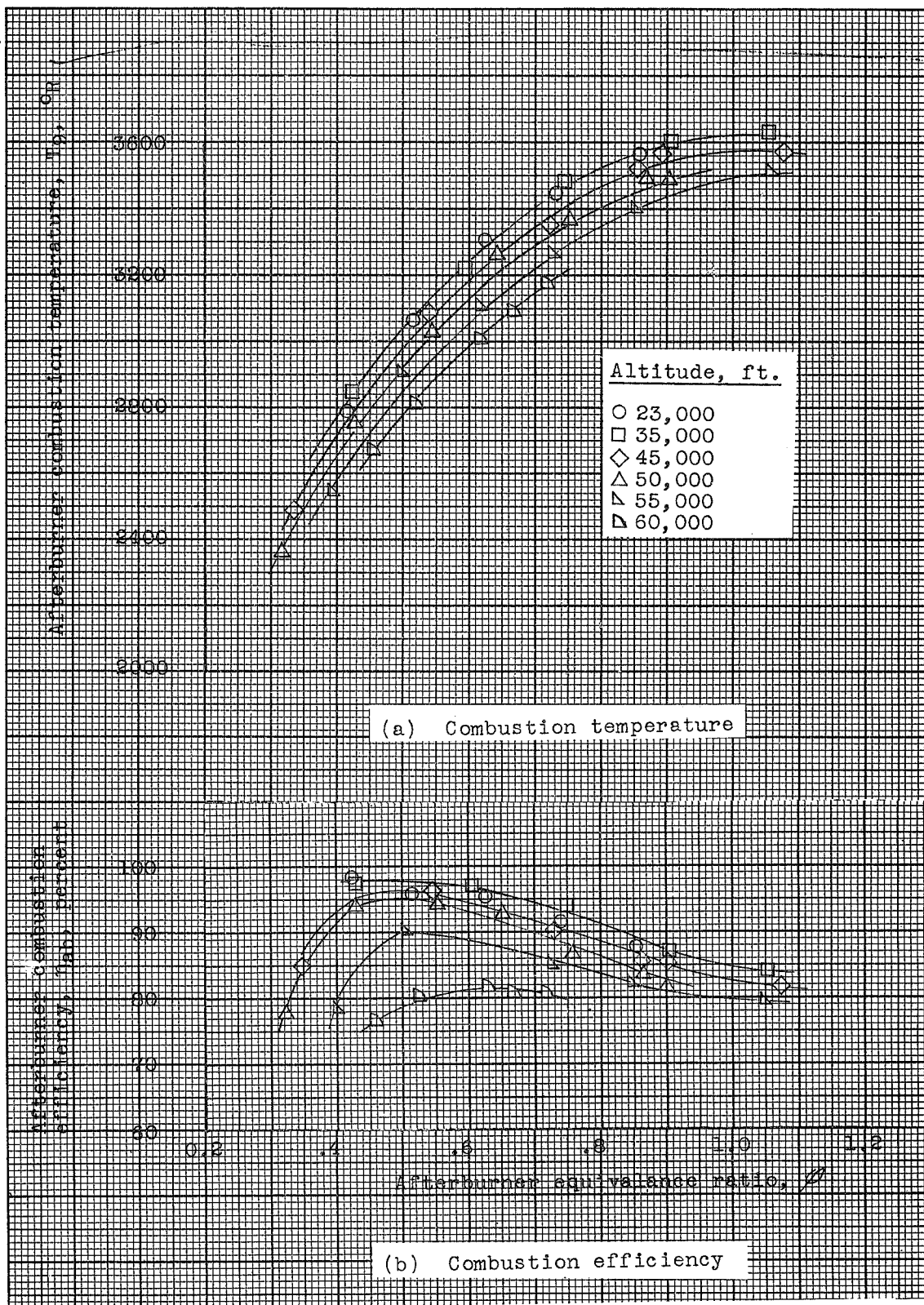


Figure 6. J71-A2 turbojet engine afterburner combustion performance variation with altitude.

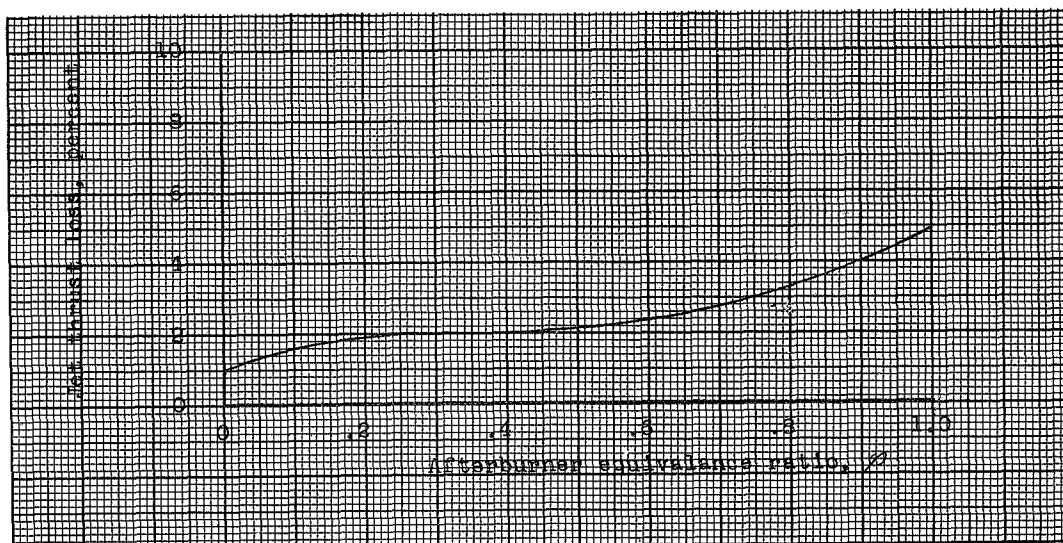


Figure 7. Jet thrust loss due to ejector configuration on J71-A2 turbojet engine afterburner. $P_9/p_0 = 3.57$

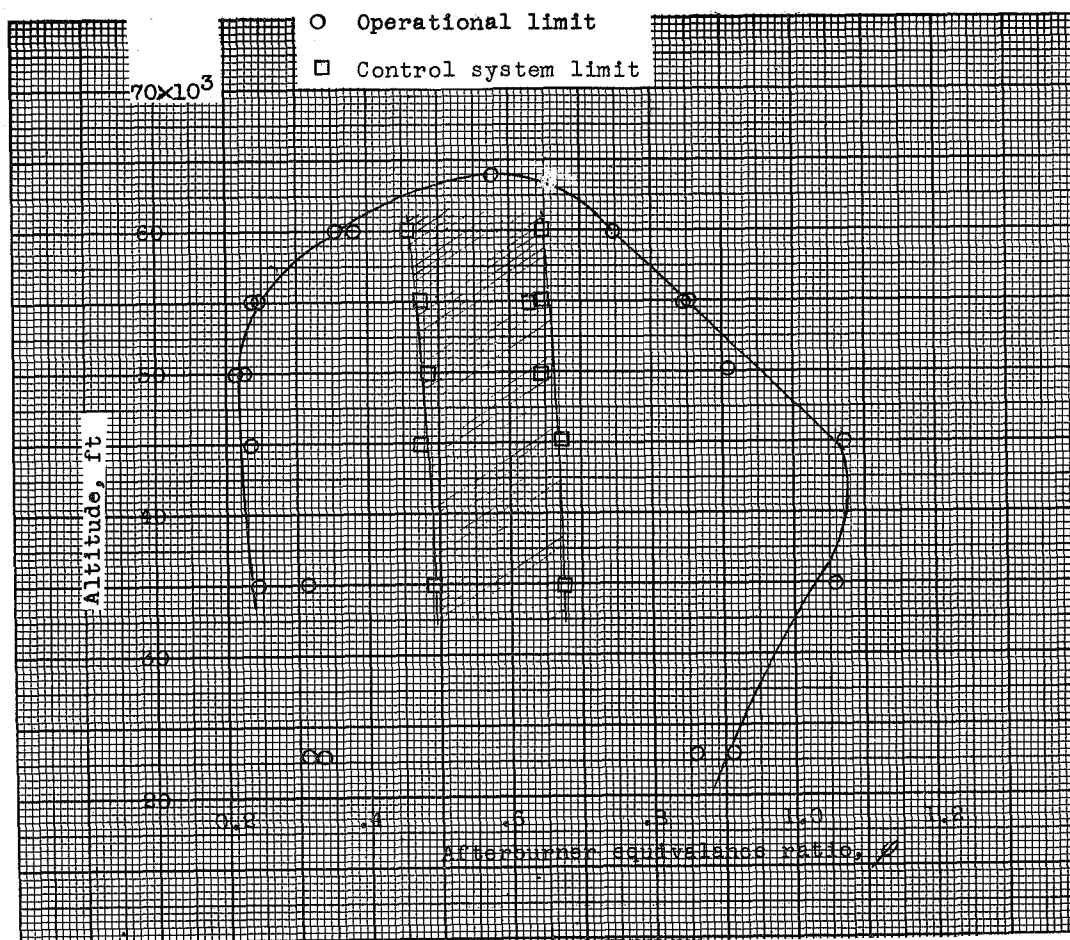


Figure 8. J71-A2 turbojet engine afterburner operational limits and afterburner control system limits of operation.

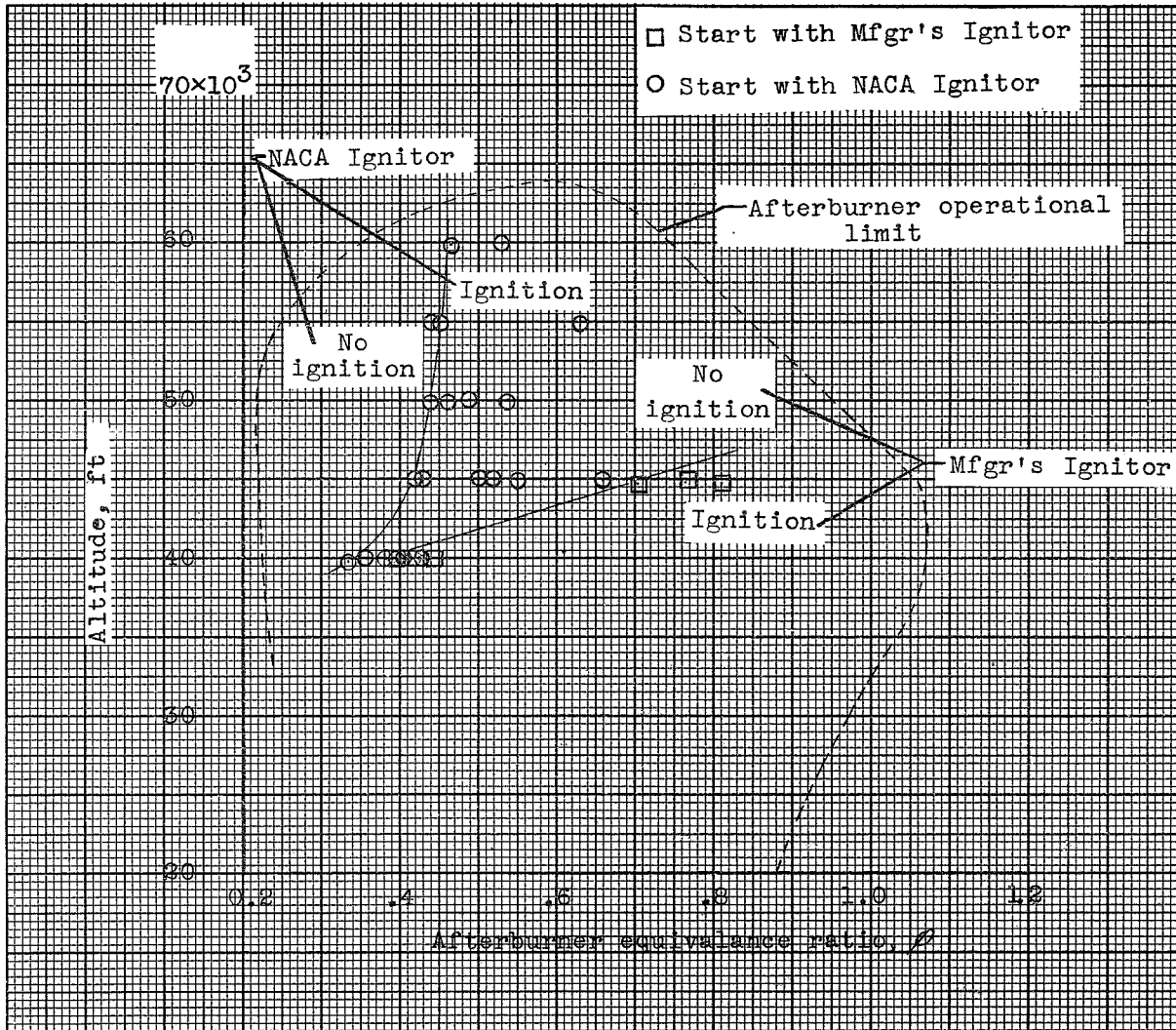


Figure 9. Area of afterburner ignition using the manufacturer's ignitor and the NACA "hot streak" ignitor.

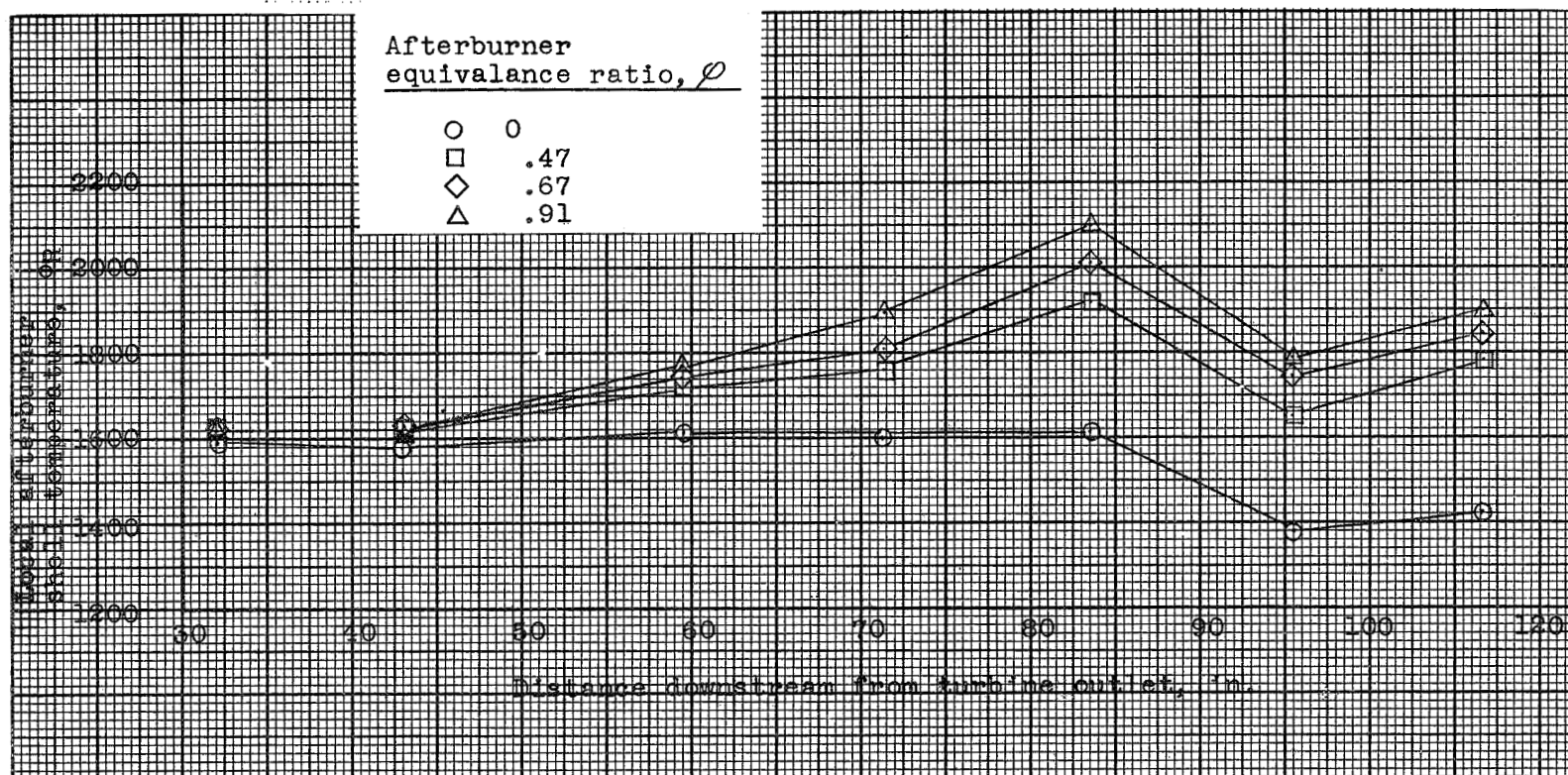
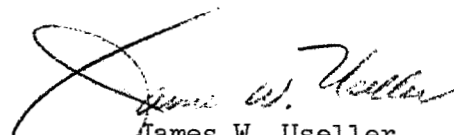


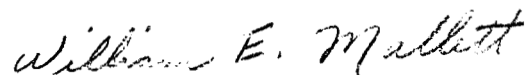
Figure 10. Local afterburner shell temperature distribution along length of the afterburner during operation at several equivalence ratios.

PRELIMINARY ALTITUDE PERFORMANCE DATA OF J71-A2

TURBOJET ENGINE AFTERBURNER

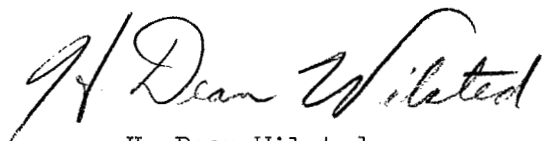


James W. Useller
Aeronautical Research Scientist
Propulsion Systems

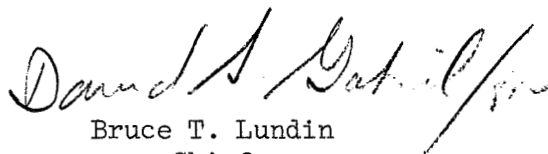


William E. Mallett
Aeronautical Research Scientist
Propulsion Systems

Approved:



H. Dean Wilsted
Aeronautical Research Scientist
Propulsion Systems



Bruce T. Lundin
Chief
Engine Research Division

NACA RM SE54J06

~~CONFIDENTIAL~~

FORWARD

To permit expeditious transmittal of performance data to those concerned, figures and a tabulation of "Preliminary Data" are presented herein. Preliminary Data are test data that have not received the complete analysis and extensive cross-checking normally given a set of NACA data before release.